Activated Carbon-Filled Cellulose Acetate Hollow-Fiber Membrane for Cell Immobilization and Phenol Degradation

GUANHUA ZHU,[1] TAI-SHUNG CHUNG,[1 2] KAI-CHEE LOH[1]

[1]Department of Chemical and Environmental Engineering, National University of Singapore, 10 Kent Ridge Crescent, Singapore 119260

[2]Institute of Materials Research and Engineering, 10 Kent Ridge Crescent, Singapore 119260

Received 22 April 1999; accepted 5 August 1999

ABSTRACT: The activated carbon-filled cellulose acetate (CA) hollow-fiber membranes were prepared by using phase-inverse technique and subsequently characterized by scanning electronic microscopy (SEM), atomic force microscopy (AFM), dynamic mechanical analysis (DMA), thermal mechanical analysis (TMA), and tensile analysis. The SEM observation demonstrated that the activated carbon-filled CA hollow-fiber membranes possess four-layer structure, which consists of an external skin dense layer, an external void layer, a central sponge layer, and an internal skin dense layer, whereas the pure CA hollow-fiber membranes lack the macrovoid layer. As the measurement of AFM, the roughness of both internal and external surface of activated carbon-filled fibers is much higher than that of pure CA fiber, respectively. Higher Young's modulus and storage modulus of filled membranes indicate that the activated carbon particles were homogeneously dispersed in the polymeric matrix. To investigate the feasibility of the newly developed hollow-fiber membranes for cell immobilization cells and to evaluate the inhibitory effect of phenol on immobilized cells, *Pseudomonas putida* ATCC 17484 was chosen to be immobilized on both pure CA and activated carbon-filled hollow-fiber membranes. Batch experiments for phenol biodegradation were carried out for both free suspension and immobilized cells at the initial concentration of 1500 mg/L phenol. In the case of free suspension, neither cell growth nor phenol degradation occurred to any measurable extent up to 35 h. We found that both pure CA fiber and activated carbon-filled fiber immobilization systems can completely degrade the phenol. However, the biodegradation rate of activated carbon-filled fiber system was higher than that of pure CA fiber system. © 2000 John Wiley & Sons, Inc. J Appl Polym Sci 76: 695–707, 2000

Key words: activated carbon; cellulose acetate; hollow-fiber membrane; cell immobilization; phenol

INTRODUCTION

A number of industrial processes produce phenolic wastewater in which phenol may be present at a concentration as high as several grams per liter. Because of their toxicity and persistence, inadequate handling of the wastewater will lead to a serious pollution problem. Biological treatment of industrial effluents and bioremendation of the contaminated environment by exploiting the capability and potential of microorganisms have been considered the most promising approaches. Microorganisms exhibit fascinating metabolic diversity and ability to evolve rapidly

Correspondence to: T.-S. Chung (chencts@nus.edu.sg).

Contract grant sponsor: The National University of Singapore and The Environmental Technology Enterprise; contract grant numbers: PR 960609A and RP 3602037.

Journal of Applied Polymer Science, Vol. 76, 695–707 (2000)

new catabolic properties for the degradation of xenobiotics. Hence, many bacteria have been isolated and/or induced to degrade phenol, in which microoganisms use phenol as a carbon and energy source for growth.[1–5] However, these bacteria can only grow optimally at a phenol concentration of about 50–100 mg/L, whereas their growth is inhibited at a higher concentration of phenol.[6,7] To reduce the inhibitory effects of phenol and maintain a continuous bacteria growth at present of higher concentration of phenol, it is necessary to construct a barrier between the phenol and the bacteria so that phenol degradation can still be effected without the effect of substrate inhibition. Immobilization of cells has the potential application to meet this requirement.

Immobilization of cells means that the cells have been confined or localized so that it can be reused continuously.[8] The use of immobilized cells may offer several advantages over processes with suspended biomass, such as retention of a higher concentration of microorganisms in the reactor, protection of cells from toxic substrates, and separation of suspended biomass from the effluent.[9] The cells may be immobilized in or on a variety of materials, including alginate beads,[9,10] diatomaceous earth,[11] ionic network polymer,[12] activated carbon (AC),[13] sintered glass,[14] polyacrylamide beads,[15] and hollow-fiber membrane.[6,7] Bettman and Rehm[15] found that *Pseudomonas* cells immobilized in alginate and polyacrylamide hydrazide showed higher degradation rates of phenol in wastewater than free cells. Moreover, the immobilized bacteria possessed an increased resistance against the xenobiotics. Keweloh and his coworkers[16] studied the phenol tolerance of free and immobilized cells of *Escherichia coli, Staphylococcus aureus*, and *Pseudomonas putida* p8. Among the three strains, only *P. putida* was able to use phenol as a substrate for cell growth, but all strains showed higher phenol tolerance after immobilization. They, therefore, concluded that the tolerance enhancement is a general characteristic of immobilization, which may be attributed to the formation of cell colonies in the immobilization materials. The close cell-to-cell contact influences the dynamics of the cell membrane and thus increases the cell's tolerance to xenobiotics. It is obvious that the immobilization of microorganisms has a great advantage in the treatment of wastewater, which consists of substances of antimicrobial activity or contains toxic chemicals in high concentration.

ACs are porous carbonaceous materials made from various raw materials (coal, wood, polymers). Their internal porous volume and pore size are strongly dependent on the raw material used and the manufacturing process (i.e., the activation conditions). The internal surface area can reach up to 1500 m^2/g and a porous volume of 2 cm^3/g.[17] ACs show a high preferential adsorption selectivity for aromatic compounds in solution, especially in the low concentration range of the aromatic compound. From the literature, the adsorption of phenol on powdered ACs followed a typical Freundlich isotherm.[18] Mörsen and Rehm[14] investigated the degradation of phenol by a defined mixed culture of the yeast *Cryptococcus elinovii* H1 and the bacterium *Pseudomonas putida* P8 immobilized by adsorption on AC and sintered glass, respectively. The results showed that the AC system could completely degrade 17 g/L in batch culture, whereas the sintered glass system was able to degrade phenol up to 4 g/L. The authors claimed the AC seems to be better suited to serve as a carrier for the immobilization of microorganism in the treatment of wastewater where a high concentration of pollutants are present because AC compared to sintered glass possesses the ability to work as a buffer by adsorbing high phenol concentrations immediately and subsequently protect adsorbed microorganisms against damage by phenol.

Membrane acts as a barrier to prevent mass movement but allows restricted and/or regulated passage of one or more species through it. Polymeric hollow-fiber membranes with varied and complex porous microstructure are prepared by phase inversion in spinning process. By using this technique, membranes for gas separation, reverse osmosis, ultrafiltration, and microfiltration have been produced from a variety of materials including cellulose derivatives, polyamides, polyimides, and polysulfones. Phase inversion is commonly brought about by solvent exchange between the nascent fiber and internal and external coagulants. A hollow fiber is formed when the as-spun fiber is fully precipitated. The resultant membrane microstructure is dependent on the kinetics and thermodynamics of solvent exchange mechanism as well as elongational stresses, solid concentration, and air-gap distance during the fiber spinning process.[19] In previous studies, Chung et al.[6,7] fabricated cellulose acetate (CA) and polysulfone (PS) hollow-fiber membranes to immobilize *Pseudomonas putida* ATCC 49451 for the biodegradation of high phenol concentrations in wa-

Table I Spinning conditions for cellulose acetate hollow fibre membranes

	Pure CA Membrane	Activated Carbon Filled Membrane
Cellulose acetate (g)	40	38
Acetone (g)	112	112
N-methyl-2-pyrrolidone (NMP) (g)	48	48
Activated carbon (g)	0	2.0
Coagulant (internal and external)	Water	Water
Length of air gap (cm)	0	0
Extrusion pressure (psi)	20	20
Internal coagulant flow rate (ml/min)	0.1	0.1
Speed of take-up roller (m/min)	1.0	1.0

ter. They found that both CA and PS hollow-fiber membranes developed were suitable for cell entrapment. The results showed that entrapping the bacteria in the membranes not only shielded them from direct contact with the toxic high phenol concentration, but their tolerance to phenol was also increased.

Introducing absorbents into a polymer membrane-forming system offers the opportunity for the development of complex polymer composite particular for separation process.[20] In the last decades, the incorporation of fillers into polymer matrix to fabricate composite flat membranes for liquid separation, pervaporation, and gas separation has gained increasing attention in literature.[21–28] A variety of absorbents such as zeolites, molecular sieves, and ACs were used as fillers. However, there is no report about the fabrication of hollow-fiber membrane, although Zimmerman et al.[29] theoretically studied the mixed matrix composite hollow-fiber membrane for gas separation. The authors stated that mixed matrix composite membranes, incorporating molecular sieving materials within polymeric substrates, might provide economical high-performance gas separation membranes if defects at the molecular sieve/polymer interface could be eliminated.

The objective of this work is to develop the activated carbon-filled cellulose acetate composite hollow-fiber membranes for immobilizing the bacteria to enhance phenol tolerance of bacteria. The morphology, mechanical properties, thermal properties, and permeability of the developed hollow fiber were measured. The sorption behavior of phenol on hollow-fiber membrane was investigated. The immobilization of *Pseudomonas putida* ATCC 17484 on hollow-fiber membranes and the degradation of higher concentration phenol by immobilized cells were also studied.

EXPERIMENTAL

Fabrication of Hollow-Fiber Membranes

Materials

CA (type HB-105) was kindly supplied by Hoechst Celanese (Rock Hill, SC). *N*-methyl-2-pyrrolidone (NMP), acetone, and methanol were purchased from Merck (Rahway, NJ) and used as received. Granular AC (type F-400) was purchased from Calgon Carbon Corp. (Pittsburgh, PA). The ACs had to be ground before incorporation into polymeric matrix. The size of AC was measured by Analysette 22 laser particle sizer. The average size of the AC is about 7.8 μm.

Spinning Process

A 20 wt % solid dope was prepared in a binary solvent system consisting of NMP and acetone. The weight ratio NMP and acetone was 30 : 70. Acetone is a common solvent for CA. Because it is highly volatile, a second solvent NMP was added to suppress its vaporization and to maintain the stability and shelf life of spinning solutions.

The spinning process has been well described in detail elsewhere.[6,7] Wet spinning was used to spin the hollow fibers. The spinning conditions we used was shown in Table I. Water was both the internal and external coagulant. The formulated dope was fed under nitrogen pressure and bore fluid was fed by 500D syringe pumps from ISCO. The spinning dope and the bore fluid met at the tip of the spinneret, which was immersed in the coagulation bath. After formation of the hollow fibers, they were stored in a water bath for at least 1 day and then transferred to a tank containing fresh methanol for at least 1 h to remove the residual NMP completely.

Characterization of Hollow-Fiber Membranes

Morphology

Hollow-fiber membrane samples for scanning electron microscopy (SEM) study were first cryogenically fractured in liquid nitrogen and then sputtered with gold of 20–30 nm thickness by using a Jeol JFC-1100 E ion sputtering device. We employed a Hitachi *S*-4500 field emission SEM to investigate the membrane morphology.

The atomic force microscope (AFM) was used to study the roughness and morphology of internal and external surface of as-spun hollow-fiber membranes. The scanning was carried out in contact mode by Topometrix Explorer 2000 with silicon nitride tips. The surface roughness was determined by Topometrix imaging software.

Mechanical Properties

Tensile properties of hollow-fiber membranes were measured at 50-mm gauge length with a drawn speed of 10 mm/min using an Instron 5542 material testing instrument in an environment of 25°C and 75% relative humidity. Each datum was obtained from the average value of five tests for each sample. The main parameters of interest are (1) fiber strength (MPa) (calculated based on the solid cross section area) and elongation (%) at break; and (2) Young's modulus (MPa), which is the slope of stress–strain curve before yield point.

Thermal Properties

Coefficient of thermal expansion (CTE), glass transition temperature (T_g), storage modulus, and loss modulus of developed hollow-fiber membranes were measured by using Thermal Instruments' thermomechanical analyzer (TMA 2940) and Thermal Instruments' dynamic mechanical analyzer (DMA 2980). When using TMA, the hollow-fiber sample was heated from room temperature to 220°C at a heating rate of 5°C/min. The dimensional change of the sample was observed as a function of temperature. When employing DMA, the hollow-fiber sample was heated from room temperature to 220°C at a heating rate of 3°C/min and a frequency of 1 Hz.

Module Fabrication and Gas Permeation Tests

Each membrane module was comprised of a bundle of four fibers with a length of 15 cm. One end of the bundle was sealed with a 5-min rapid solidified epoxy resin, while the shell side of the other end was glued into an aluminum holder using a regular epoxy resin. The prepared module was fitted into a stainless steel pressure cell for gas permeation measurement.

The permeances of gases through the hollow-fiber module were determined by using a bubble flowmeter and calculated by using the following equation:

$$\left(\frac{P}{L}\right)_i = \frac{Q_i}{\Delta P \times A}$$

where $(P/L)_i$ is the permeance of hollow-fiber membrane to gas I; GPU is used as the gas permeation units; 1 GPU is equal to 1×10^{-6} cm^3 (STP) cm^{-2} s^{-1} cmHg^{-1}; Q_i is the volumetric flow rate of gas i at standard temperature and pressure (ml/s); ΔP is the transmembrane pressure drop (cmHg); and A is the membrane surface area. The selectivity of gas i to gas j is calculated as:

$$\alpha_{ij} = \frac{(P/L)_i}{(P/L)_j}$$

Sorption Studies

The adsorption isotherm for phenol on AC was obtained by adding a given amount of AC to a flask containing a given amount of phenol solution at 25°C until equilibrium state was reached. Equilibrium was achieved within about 1 week. After equilibrium, all samples were filtered prior to analysis to eliminate interference from the carbon fines in the supernatant. Similarly, hollow fibers of known weight were immersed in phenol aqueous solutions of different known concentrations and weight. After equilibrium, the hollow fibers were removed and weighed after the superfluous liquid was wiped with tissue paper. The increase in weight is due to phenol and water taken up by the hollow fiber. The supernatant liquid was analyzed on UV spectrophotometer at a wavelength of 270 nm. The amount of the phenol adsorbed on the AC and hollow fiber was then calculated by materials' balance.

Cell Culture and Phenol Degradation

The culture conditions and immobilization have been well described in previous studies.[6,7] The microorganism used throughout this work was a pure culture of *Pseudomonas putida* ATCC 17484. Stock cultures *of P. putida* were main-

tained by periodic subtransfer on nutrient agar slants, which were stored at 4°C. All batch cultures were carried out in 500-mL Erlenmeyer flasks with a cotton plug at 250 mL medium volume. The mineral salt medium contained (g/L): K_2HPO_4, 4.36; $NaH_2PO_4H_2O$, 3.45; NH_4CL, 1.0; $MgSO_47H_2O$, 0.48; $CaCl_22H_2O$, 0.036; $(NH_4)_6Mo_7O_{24}4H_2O$, 0.0002; $FeSO_47H_2O$, 0.002; $MnCl_24H_2O$, 0.001; $CoCl_26H_2O$, 0.001. The sole carbon source, phenol (analytical grade; Merck, Darmstadt, Germany), was added accordingly to obtained the desired concentration for batch operation.

All media (except phenol), pipette tips, hollow-fiber membranes (in immobilization studies), and Erlenmeyer flasks fitted with cotton plugs were autoclaved at 121°C for 20 min before inoculation. Culture transfers and sampling were conducted aseptically around a Bunsen flame to minimize contamination. *P. putida* was activated in a medium containing 200 mg/L of phenol. Activated cells in the late exponential growth phase were harvested as inoculum for the experiments. The late exponential growth phase was evident from the change in medium color to a distinctive yellowish-green as well as an optical density (OD) of 0.35–0.40 absorbance units.

Free suspension cultivation was conducted by inoculating 2 mL of activated *P. putida* into 250 mL of culture medium with phenol concentration of 300 mg/L. After inoculation, the flask was capped with cotton plugs and placed on water bath rotary shakes at 150 rpm and 30°C. Cells at late exponential phase were harvested by centrifugation at 12,000 rpm for 15 min. The spent medium at the top was discarded and the biomass pellets at the bottom were rinsed with a mineral solution and then centrifuged three times. The harvested cells were made up to an OD of 0.9 absorbance units with mineral salt medium. Cell suspension (30 mL) was added to a flask containing 15 fibers 15-cm long. The flask was agitated in the water bath rotary shaker for 16 h to allow cells to diffuse into the membranes for immobilization. After that, the fibers were taken out of the solution and rinsed with deionized water to remove surface cells. The rinsed fibers were placed in fresh medium containing phenol at 1500 mg/L. All phenol degradation experiments were conducted in duplicate.

Analytical method for cell density and phenol concentration follows previous study.[30] Samples were taken for analysis of cell density and concentrations of phenol at regular intervals. Cell density was monitored spectrophotometrically by measuring the absorbance at a wavelength of 600 nm. The phenol concentration was analyzed by gas chromatography (GC) (Model 8700; Perkin–Elmer, Palo Alto, CA). The average biodegradation rate of phenol was calculated by dividing the net amount of transformed phenol for the time period when phenol were about 10 and 90% of the initial phenol by the corresponding elapsed time.[30]

RESULTS AND DISCUSSION

Morphology of Hollow-Fiber Membranes

The scanning electronic microscope (SEM) observation was performed to study the structure and morphology of hollow-fiber membranes. Figure 1 (a, b) shows the cross section view of pure CA and activated carbon-filled CA hollow-fiber membranes, respectively, prepared from wet-spun technique under the spinning conditions, which were summarized in Table I. The pure CA hollow-fiber membrane [Fig. 1(a)] is comprised of three layers with different pore sizes: thinner outer and inner layers have smaller pores, whereas the central sponge-like supporting layer has slightly larger pores. These results are consistent with the previous studies.[6] In contrast, the CA hollow-fiber membrane with 5 wt % AC loading has a four-layer structure, which consists of an external skin layer, an external void layer, a central sponge layer, and an internal skin layer. The external and internal skin layers of the activated carbon-filled CA hollow-fiber membrane were the densest layers in the cross section as evident in Figure 2(a, b). The external fingerlike macrovoid layer had highly porous fingerlike void structure with the pore size of about 5 μm, which presents low hydrodynamic resistance to liquid flow and thus resulted in high membrane permeability. In the wet spinning processing, a large amount of solvent has to be leached out from dope solution, which results in tremendous shrinkage and local imbalance during the solvent exchange. These stresses are part of the driving forces to produce finger voids.[19] The central sponge layer provided support and added strength to the overall membrane. Figure 2(a) gives a closer view of microvoids the length of which is approximately 8 μm. Figure 2(b) shows high magnification image of the cross section near to the inner skin layer. The pore size of the sponge layer was estimated to be

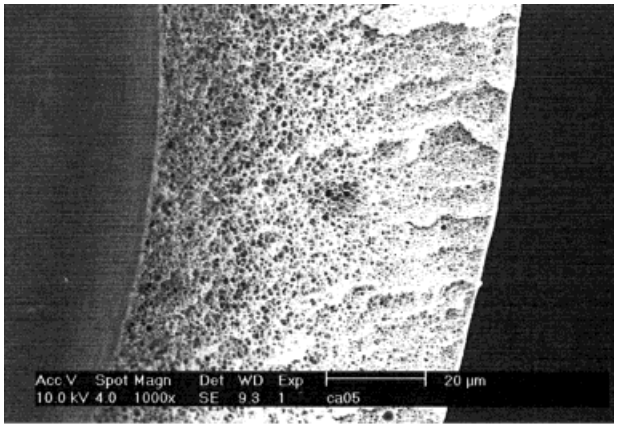

a

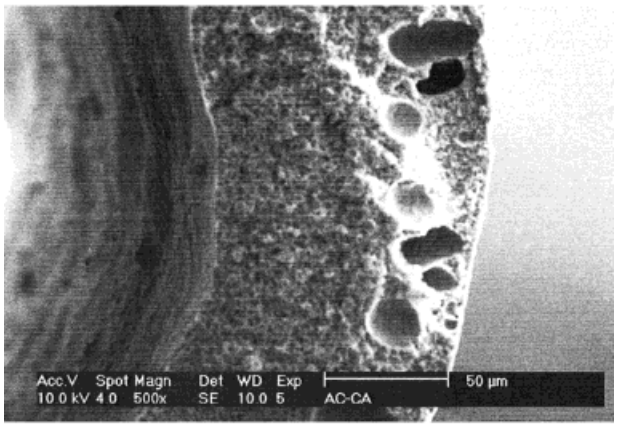

b

Figure 1 Cross section SEM pictures of hollow-fiber membranes: (a) pure CA membrane; (b) activated carbon-filled membrane.

approximately 1.0 μm. Figure 2(b) also shows that the AC particle with the size of about 6 μm was embedded in the spongelike polymer matrix.

AFM has become a very important tool in surface analysis on various fields such as biological science and materials engineering. AFM has a cantilever equipped with a very sharp tip, which extends vertically from the free end of the cantilever. While scanning, the sharp tip scans over the sample surface, and the cantilever was deflected by the different surface features. The topographical image of the surface was obtained from the deflections of the cantilever. The AFM topographical images of internal and external surface of as-spun fibers were shown in Figures 3 and 4, respectively. It can be found that both the pure CA and activated carbon-filled membranes show smooth internal surface with some irregular defects. The external surface of pure CA membranes exhibited flat and smooth with some round holes, the diameter of which was approximately 1 μm. However, the external surface of the activated carbon-filled surface was rough and heterogeneous and showed many granular particles on the surface. This phenomenon may be due to the imcompatibility between rigid AC particles and flexible CA.

Root-mean-square roughness of the fiber surface, which is defined as the standard deviation of the height values within the given area, was calculated from AFM images. Table II gives the roughness of internal and external surface of as-

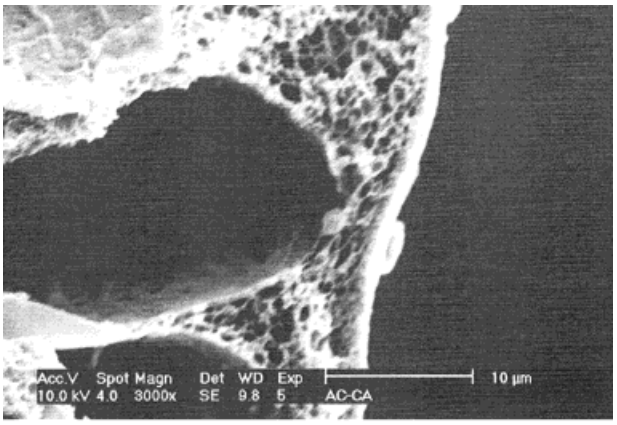

a

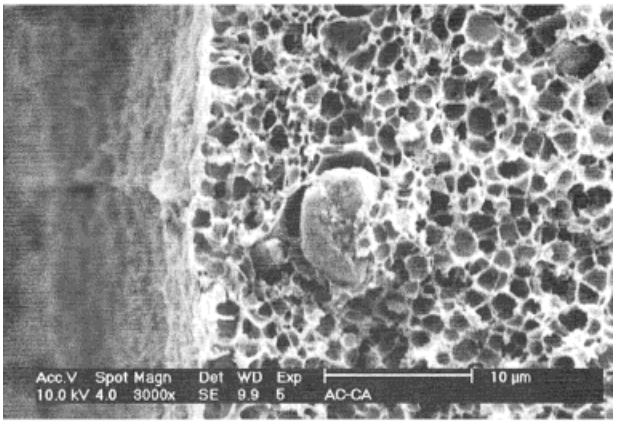

b

Figure 2 High-magnification SEM pictures of activated carbon-filled membrane: (a) near external edge; (b) near internal edge.

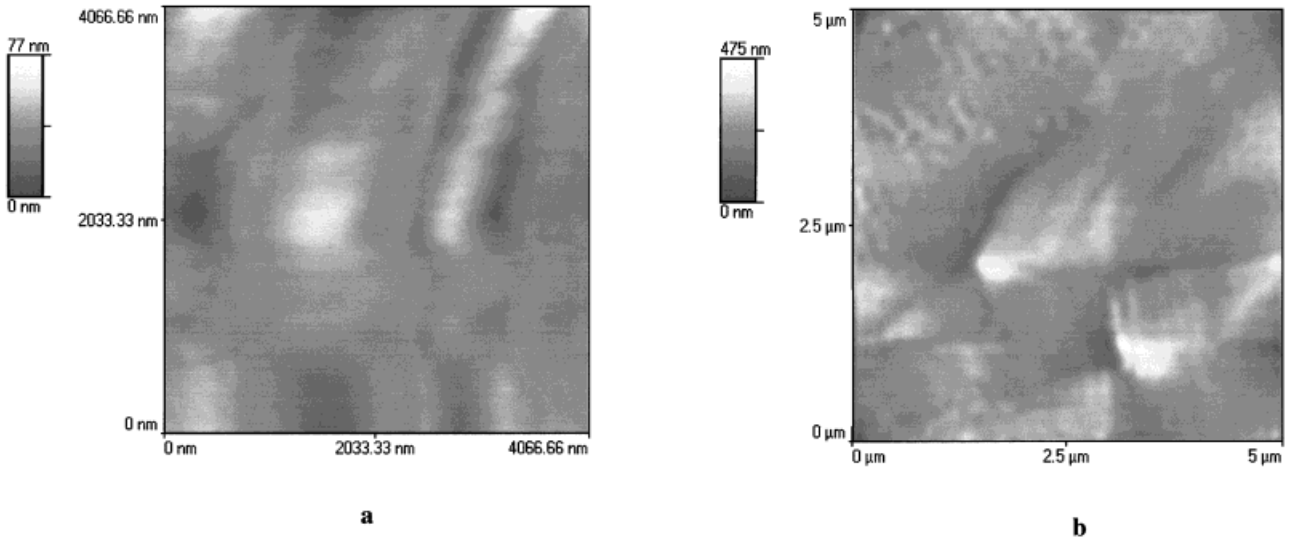

Figure 3 AFM topographical images of hollow-fiber membrane internal surface: (a) pure CA; (b) activated carbon-filled.

spun fiber. It can be noted that, for both pure CA fiber and activated filled carbon fiber, the roughness of external surface is higher than that of internal surface. The roughness of internal and external surface of activated carbon-filled fiber is almost four times than that of pure CA fiber, respectively.

Gas Permeability, Mechanical, and Thermal Properties

Although the objective of this work is not to develop hollow-fiber membranes for gas separation uses, the gas separation performance in terms of permeation flux and permselectivity was measured to further understand and characterize the membrane structure. The O_2 permeance of activated carbon-filled membranes is 137.4 GPU, which is much larger than that of pure CA membranes (23.2 GPU).[6] This phenomena is due to the fact that the activated carbon-filled membrane has the microvoid fingerlike layer [Fig. 1(b)] and its internal and external skin layers are thinner than those of pure AC membrane. The porosity of this membrane may be similar to the microfiltra-

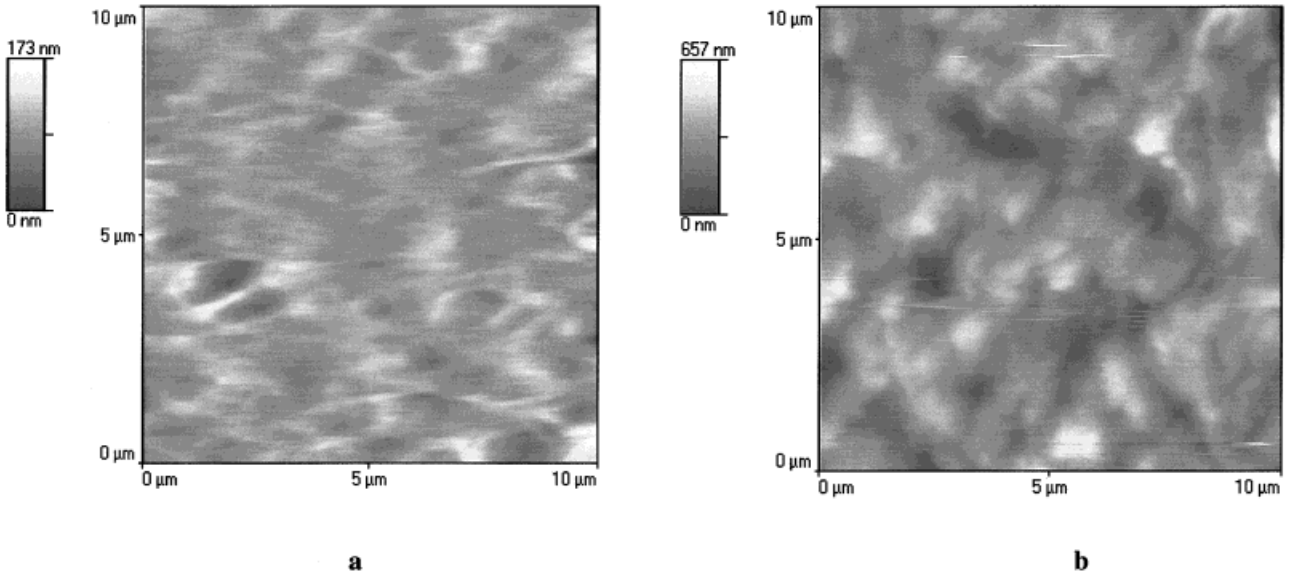

Figure 4 AFM topographical images of hollow-fiber membrane external surface: (a) pure CA; (b) activated carbon-filled.

Table II Break strength, elongation and Young's modulus of hollow fibre membranes

	Roughness (nm)	
	External Surface	Internal Surface
Pure CA	29.76	9.33
Activated carbon filled	125.00	52.27

tion membrane. The permselectivity of O_2/N_2 suggests that activated carbon-filled membrane exhibits some of Knudsen flow characteristics (i.e., separation factors α_{O_2/N_2} is < 1 and is approximately 0.90).[31]

The effect of AC loading on hollow-fiber membrane's strength, break elongation, and Young's modulus is shown in Table III. The Young's modulus, or modulus of elasticity, may be considered as stiffness, or material's resistance to elastic deformation. Both the Young's modulus and the break strength of the activated carbon-filled membrane were higher than those of the pure CA membrane. The increase in Young's modulus and strength may be due to the reinforcement effects as the rigid AC and CA-formed composite. However, there is no significant difference of elongation at break between activated carbon-filled membrane and pure CA membrane because the AC loading is very low.

DMA experiments were performed on both pure CA and activated carbon-filled fibers. Dynamic storage modulus is one of the most important properties to assess the load-bearing capability of a material. Figure 5 depicts DMA curves of the storage modulus versus temperature of pure CA fibers and activated carbon-filled CA fibers. The curves indicate that the storage modulus values of activated carbon-filled CA fibers at any temperature is higher than that of pure CA fibers because of the reinforcement effects of AC. The reinforcement effects demonstrated by both Young's modulus and storage modulus indicate that the AC particles were uniformly dispersed in polymeric matrix.

It is also evident from DMA study that the degree of modulus loss due to thermal transition is the same in two fibers. The loss modulus is associated with the dissipation of energy as heat when the material is deformed. Figure 6 plots loss moduli versus temperature of fibers with and without AC. Similar to the storage modulus curves, it can be seen from Figure 6 that loss modulus of fibers with AC is higher than that of pure CA fibers. This may be due to the fact the incorporation of AC particles into polymeric matrix restrict the movement of polymer molecule, and therefore, results in more irreversible molecular chain rearrangement and relaxation of fibers when they are subjected to heat and deformation

The T_g and CTE of the hollow-fiber membranes were measured by TMA. Each sample was tested three times and the results are reproducible. Figure 7 shows the typical curves of the dimension-changed pure CA and activated carbon-filled fibers as a function of temperature. It was found that both the CTE and T_g of activated carbon-filled membranes were slightly higher than those of pure CA membranes. T_g is always used to explain membrane structure on the molecular scale when employing a thermal analysis on a membrane.[32] A higher T_g indicates that membrane has more free volume fraction, therefore a looser structure and vice versa. In the phase-inversion process, the addition of rigid AC particles results in unoriented chain entanglement with a loose structure of membranes, which was observed by SEM. In the same fashion, a higher CTE of activated carbon-filled membranes indicates that the molecular chains of the membranes were more unoriented than those of pure CA fibers. This finding is in good agreement with the free-volume theory proposed by Kovacs[33] and Matsuoka.[34]

Table III Roughness of internal and external surface of hollow fibre membranes

Activated Carbon Loading (wt %)	OD (μm)/ID (μm)	Break Stress (MPa)	Break Strain (%)	Young's Modulus (MPa)
0	683/446	11.4 ± 0.8	37.0 ± 5.1	289.6 ± 18.1
5	679/454	13.6 ± 0.5	31.0 ± 1.8	370.3 ± 27.6

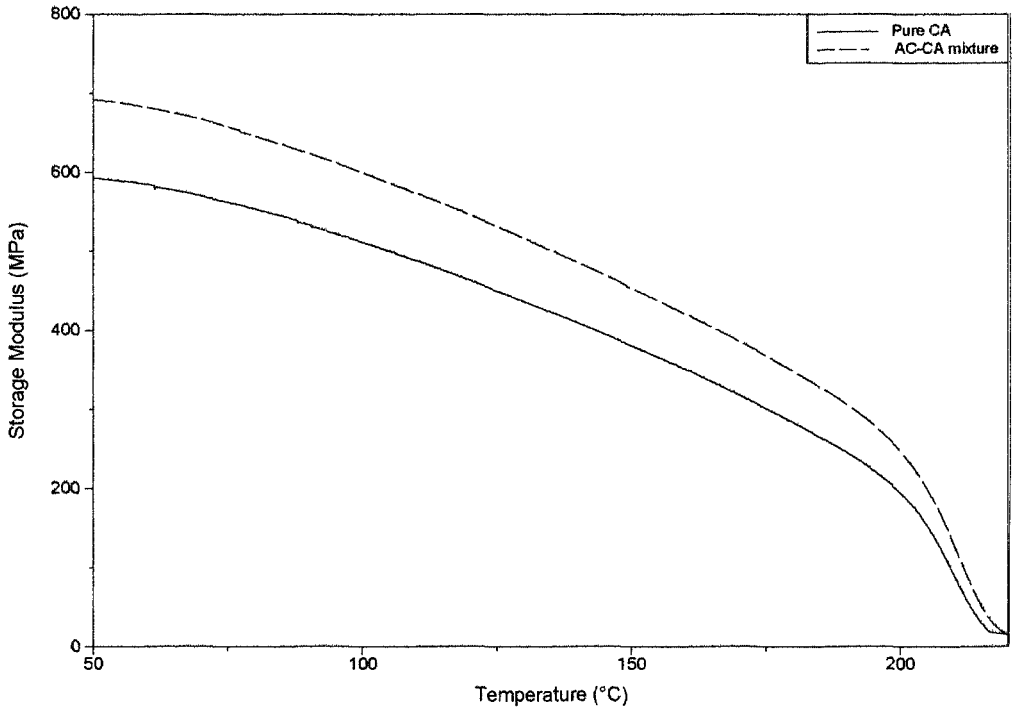

Figure 5 Dimension change of hollow-fiber membrane as a function of temperature measured by TMA: (—) pure CA; (- - -) activated carbon-filled.

Sorption of Phenol on Hollow-Fiber Membranes

Sorption is a generalized term used to describe the penetration and dispersal of penetrant molecules in a polymeric matrix to form a mixture. The sorption process can be described phenomenologically as the distribution of the penetrant between two or more phases to include adsorption, absorption, incorporation into microvoids, cluster formation, solvation-shell formation, and other modes of mixing.[35] In the sorption process, penetrant molecules may experience more than one simultaneous or sequential mode of sorption in a given polymer material. Furthermore, the distribution of penetrant between different modes of sorption may vary with sorbed concentration, temperature, swelling-induced structural states, time of sorption to equilibrium, and other factors.

Phenol sorption isotherms of ACs, pure CA fibers, and activated carbon-filled CA fibers are shown in Figure 8. It can be found that the phenol sorption capacity of AC is markedly higher than that of hollow-fiber membranes because the ACs are sorption selective for aromatic phenol in a mixture with water. Therefore, the addition of AC results in the slight increase of phenol sorption in filled membranes as shown in Figure 8.

Cell Immobilization and Phenol Degradation

It has been found that many aerobic bacteria have the ability to utilize aromatic compounds as the carbon and energy source. In the present study, *Pseudomonas putida* ATCC 17484 was chosen to investigate the cell immobilization and phenol degradation. Figure 9 shows the time profile of cell growth and phenol degradation, in which the initial phenol concentration was 300 mg/L. The cell growth exhibited the typical batch growth curve of a microbial culture, which can be chronologically divided into the lag phase, exponential growth phase, decreased growth phase, stationary phase, and death phase. Here, a short lag phase of about 4 h, where there was no appreciable cell growth and phenol degradation, was observed. After that, the cells began to grow at the expense of phenol consumption. The highest cell density (OD_{600}) was 0.58 absorbance units and phenol was completely degraded within 13 h at an average degradation rate of approximately 40 mg L^{-1} h^{-1}.

In the degradation experiment, we observed that the color of the culture medium changed from colorless to greenish-yellow after lag phase and then decolorized near the end of the experi-

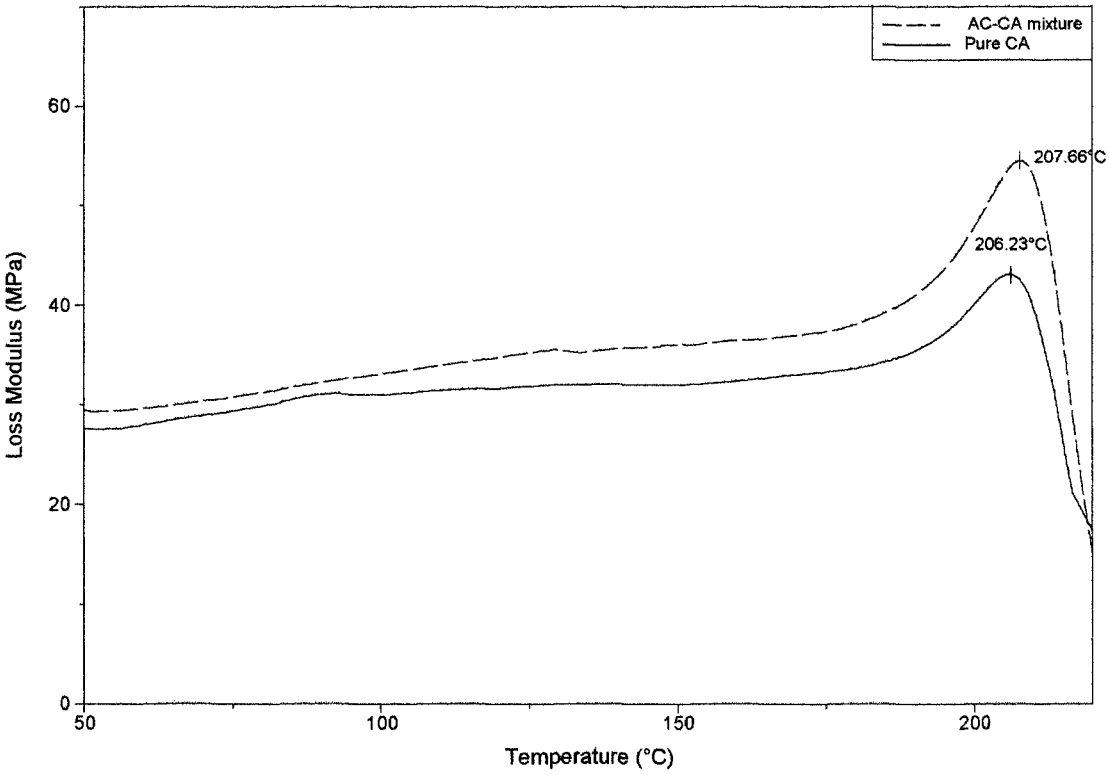

Figure 6 Storage modulus of hollow-fiber membrane as a function of temperature measured by DMA: (—) pure CA; (- - -) activated carbon-filled.

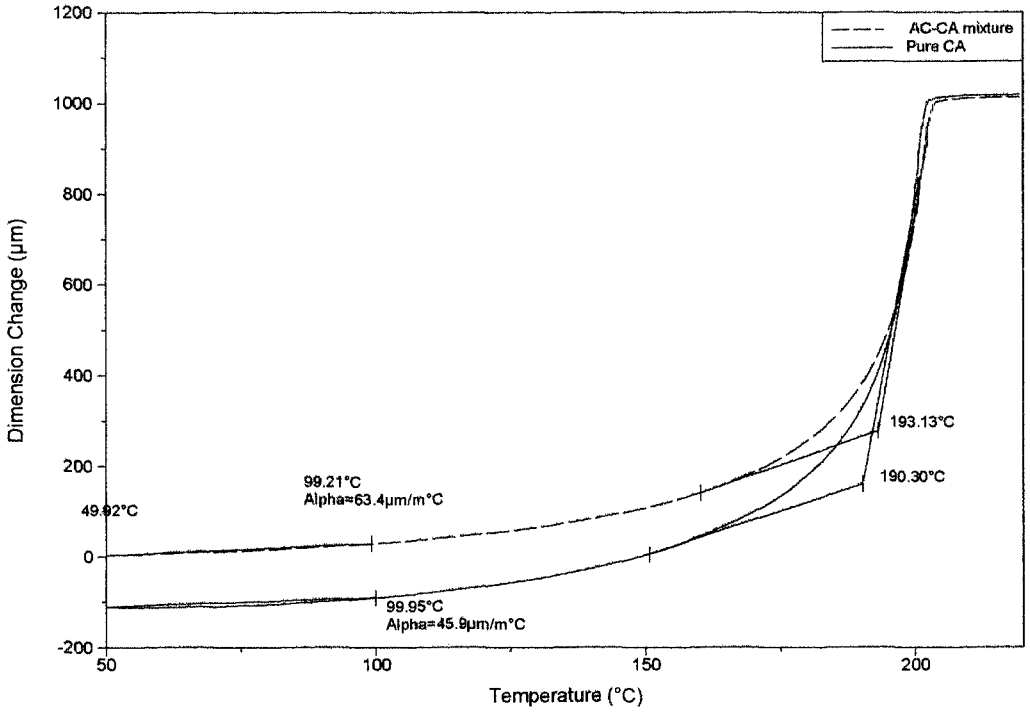

Figure 7 Loss modulus of hollow-fiber membrane as a function of temperature measured by DMA: (—) pure CA; (- - -) activated carbon-filled.

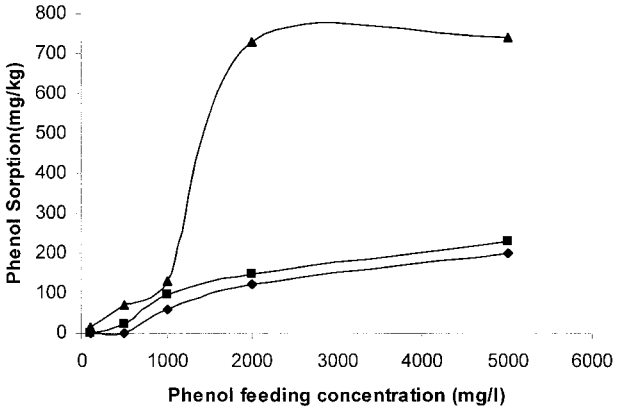

Figure 8 Phenol sorption isotherms on activated carbons and hollow-fiber membranes: (▲) pure activated carbon; (squlf) activated carbon-filled membrane; (♦) pure CA membrane.

ment. This phenomenon agrees with the observations of others[14,36] in the phenol biodegradation by *Pseudomonas* cells and indicated that cells utilize phenol through the meta pathway.[37] The change of medium color was due to the transitory formation of 2-hydroxy muconic acid semialdehyde, which was a metabolite of the *meta*-pathway degradation of phenol. The results of free suspension biodegradation of phenol show that *P. putida* ATCC 17484 is an effective strain to degrade the phenol at low concentration.

To compare the effectiveness of different hollow-fiber membranes as the immobilization substrates, batch experiments for phenol biodegradation were carried out for both free suspension and immobilized cells at the initial concentration of 1500 mg/L phenol in duplicate. The results are reproducible. Figure 10(a, b) shows cell growth and phenol concentration profile in free suspension and immobilized systems at the initial phenol concentration of 1500 mg/L. In the case of free suspension, neither cell growth nor phenol degradation occurred to any measurable extent up to 35 h. This indicated that substrate inhibition was extremely severe at 1500 mg/L phenol in the medium. In suspension culture at 1500 mg/L phenol, the bacteria were exposed to a higher toxicity caused by high phenol concentration. This toxicity of the microenvironment surrounding the cells made cell growth unfavorable, and as a result the cells eventually died. The slight decrease in the optical density of the suspension culture indicated a reduction in the cell density. These are signs of a lack of cell viability, suggesting that the cells had died over 35-h processes.

As observed from Figure 10, the data obtained in both immobilized systems, filled and pure CA fibers, were discernibly different from those obtained in the suspension culture. Although there was no phenol degradation in the suspension culture at 1500 mg/L initial concentration, the de-

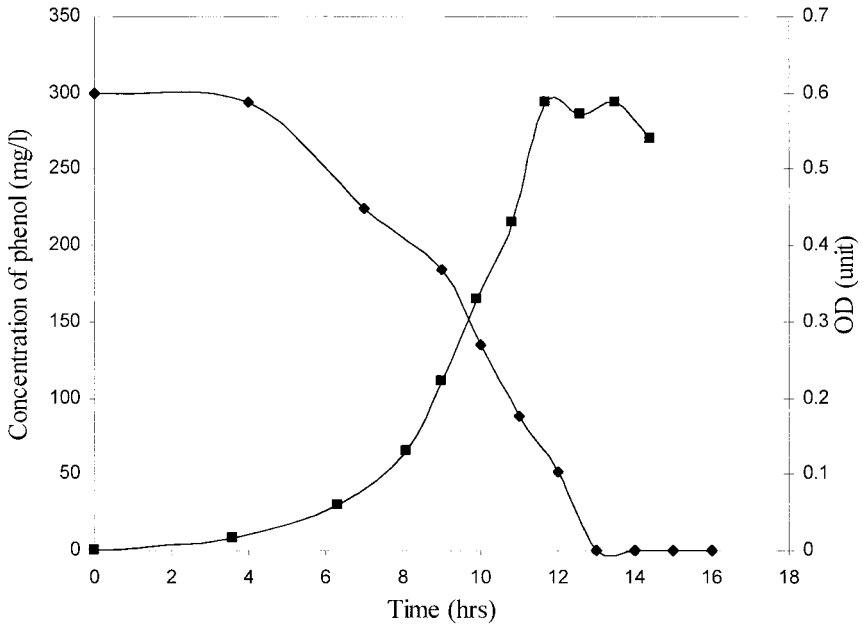

Figure 9 Cell growth and phenol degradation profile at phenol initial concentration of 300 mg/L: (■) optical density (OD); (♦) phenol concentration.

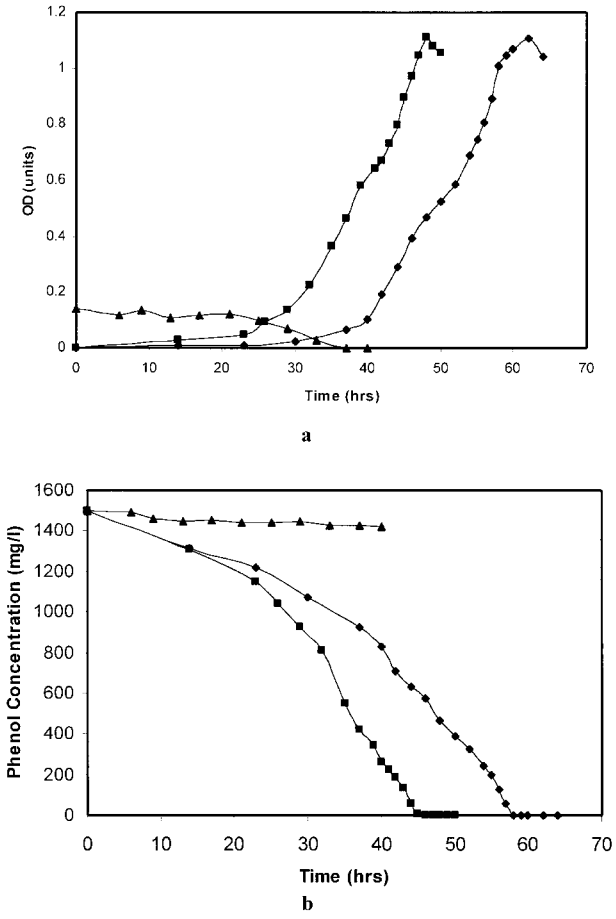

Figure 10 Cell growth and phenol degradation profile at phenol initial concentration of 1500 mg/L: (a) cell growth; (b) phenol degradation; (▲) free suspension; (♦) pure CA membrane; (■) activated carbon-filled membrane.

crease of phenol concentration in the immobilized systems was evident from the start of the experiments. It also can be seen from Figure10 that there are two stages in the phenol degradation by immobilized cells. In the first stage, the cell density in the medium was extremely low and the phenol concentration decreased slowly until 900 mg/L. During this time, phenol concentration in the liquid phase was probably reduced in two ways. One way is that the phenol was absorbed by both pure CA and filled fibers and another way is that the phenol was degraded by cells as the carbon source within the membrane. According to the sorption study, the maximum phenol sorption amount by both pure and filled CA fibers was less than the amount of phenol depletion in the liquid phase. Therefore, as well as the sorption of phenol by fibers, the immobilized cells utilized the phenol as carbon source and began to multiply within the membranes. After the phenol concentration decreased to 900 mg/L (at which concentration the substrate inhibition was not as severe as 1500 mg/L), the cells diffused into medium and survived. The cell density increased remarkably until the phenol was completely utilized, reaching a maximum optical density in the medium of 1.05 absorbance units.

We also found that phenol was completely degraded with 44 h by activated carbon-filled fiber immobilization system, whereas 58 h were needed to completely remove phenol if pure CA fiber immobilization system was employed. This may be due to the fact that the higher porosity and macrovoid structure of filled fibers make the cell growth more favorable within the membranes and phenol easier to diffuse into membranes, and therefore, increase the degradation rate of phenol at the first stage.

CONCLUSION

We successfully fabricated the activated carbon-filled CA hollow-fiber membranes by employing phase-inversion technique. The membrane wall of the activated carbon-filled fibers is composed of an external skin layer, an external microvoid layer, a spongelike layer, and an internal skin layer. The roughness of both internal and external surface of filled membranes is much higher than that of pure CA membranes, respectively. Both the Young's modulus and dynamic storage modulus of filled membranes were higher than those of pure CA membrane because of the reinforcement effects of AC particle and indicate that the AC particles were uniformly dispersed in polymeric matrix.

The batch experiments of phenol degradation demonstrated that the *Pseudomonas putida* ATCC 17484 had been immobilized on both pure CA and activated carbon-filled membrane and the phenol can be completely degraded by the immobilized cells at the initial concentration of 1500 mg/L phenol. The biodegradation rate of activated carbon-filled fiber system was higher than that of pure CA fiber system because of the higher porosity and macrovoid structure of filled fibers make the cell growth more favorable within the membranes and phenol easier to diffuse into membranes.

The authors gratefully acknowledge the financial support provided by The National University of Singapore

(NUS) and The Environmental Technology Enterprise (PR 960609A and RP 3602037). Thanks are also due to The Institute of Materials Research and Engineering (IMRE) of Singapore for the use of equipment.

REFERENCES

1. Bettman, H.; Rehm, H. J. Appl Microbiol Biotechnol 1984, 20, 285.
2. Galli, E.; Silver, S.; Witholt, B., Eds., *Pseudomonas:* Molecular Biology and Biotechnology; American Society for Microbiology: Washington, DC, 1992.
3. Ananda, S.; Chakrabarty, M.; Iglewski, B.; Kaplan, S., Eds., *Pseudomonas:* Biotransformations, Pathogenesis, and Evolving Biotechnology Silver; American Society for Microbiology: Washington, DC, 1990.
4. Raledge, C., Ed.; Physiology of Biodegradative Microorganisms; Kluwer Academic: Dordrecht, The Netherlands, 1990.
5. Ehrhardt, H. M.; Rehm, H. J. Appl Microbiol Biotechnol 1985, 21, 32.
6. Chung, T. S.; Loh, K. C.; Goh, S. K. J Appl Polym Sci 1998, 68, 1677.
7. Chung, T. S.; Loh, K. S.; Hui, L. T. J Appl Polym Sci 1998, 70, 2585.
8. Bailey, J. E.; Ollis, D. F. Biochemical Engineering Fundamentals; McGraw-Hill: New York, 1986, pp180–181.
9. Pai, S. L.; Hsu, Y. L.; Chong, N. M.; Sheu, C. S.; Chen, C. H. Bioresour Technol 1995, 51, 37.
10. Lin, J. E.; Wang, H. Y. J Ferment Bioeng 1991, 72, 311.
11. Hallas, L. E.; Adams, W. J.; Heitkamp, M. A. Appl Environ Microbiol 1992, 58, 1215.
12. Klein, J.; Hackel, U.; Wagner, F. ACS Symposium Series 106; American Chemical Society: Washington, DC, 1979, p 101.
13. Ehrhardt, H. M.; Rehm, H. J. Appl Microbiol Biotechnol 1989, 30, 312.
14. Mörsen, A.; Rehm, H. J. Appl Microbiol Biotechnol 1990, 33, 206.
15. Bettman, F.; Rehm, H. J. Appl Microbiol Biotechnol 1984, 20, 285.
16. Keweloh, H.; Heipieper, H. J.; Rehm, H. J. Appl Microbiol Biotechnol 1989, 31, 383.
17. Duval, J. M.; Folkers, B.; Mulder, M. H. V.; Desgrandchamps, G.; Smolders, C. A. Sep Sci Technol 1994, 29, 357.
18. Lee, H. W.; Kim, K. J.; Fane, A. G. Sep Sci Technol 1997, 32, 1835.
19. Chung, T. S.; Teoh, S. K.; Hu, X. J Membr Sci 1997, 133, 161.
20. Wara, N. M.; Francis, L. F.; Velamaknni, B. V. J Membr Sci 1995, 104, 43.
21. Duval, J. M.; Kemperman, A. J. B.; Folkers, B.; Mulder, M. H. V.; Desgrandchamps, G.; Smolders, C. A. J Appl Polym Sci 1994, 54, 409.
22. Gür, T. M. J Membr Sci 1994, 93, 283.
23. Jia, M. D.; Peinemann, K.-V.; Behling, R.-D. J Membr Sci 1992, 73, 119.
24. Netke, S. A.; Sawant, S. B.; Joshi, J. B.; Pangarkar, V. G. J Membr Sci 1995, 107, 23.
25. Süer, M.; Bac, N.; Yilmaz. L. J Membr Sci 1994, 91, 77.
26. Vankelecom, I. F. J.; De Kinderen, J.; Dewitte, B.M.; Uytterhoeven, J. B. J Phys Chem B 1997, 101, 5182.
27. Vankelecom, I. F. J.; De Beukelaer, S.; Uytterhoeven, J. B. J Phys Chem B 1997, 101, 5186.
28. Chen, X.; Ping, Z.; Long, Y. J Appl Polym Sci 1997, 67, 629.
29. Zimmerman, C. M.; Singh, A.; Koros, W. J. J Membr Sci 1997, 137, 145.
30. Loh, K. C.; Wang, S. J. Biodegradation 1998, 8, 329.
31. Chung, T. S.; Xu, Z. L. J Membr Sci 1998, 147, 35.
32. Chung, T. S.; Hu, X.; D. J Appl Polym Sci 1997, 66, 1067.
33. Aklonis, J. J.; Kovacs, A. J. in Contemporary Topics in Polymer Science, Vol. 3; Shen, M.; Ed.; Plenum: New York, 1971.
34. Matsuoka, S. Polym Eng Sci 1981, 21, 908.
35. Rogers, C. E. in Polymer Permeability; Comyn, J., Ed.; Elsevier: New York; 1985, pp 11–73.
36. Sala-treat, J. M.; Evans, W. C. Eur J Biochem 1971, 20, 400.
37. Yang, R. D.; Humphrey, A. E. Biotechnol Bioeng 1975, 17, 1211.